

Influence of the Gould Belt on Interstellar Extinction

G. A. Gontcharov*

May 26, 2022

Pulkovo Astronomical Observatory, Russian Academy of Sciences, Pulkovskoe sh. 65, St. Petersburg, 196140 Russia

Key words: Galaxy (Milky Way), spiral arms.

A new analytical 3D model of interstellar extinction within 500 pc of the Sun as a function of the Galactic spherical coordinates is suggested. This model is physically more justified than the widely used Arenou model, since it takes into account the presence of absorbing matter both in the layer along the equatorial Galactic plane and in the Gould Belt. The extinction in the equatorial layer varies as the sine of the Galactic longitude and in the Gould Belt as the sine of twice the longitude in the Belt plane. The extinction across the layers varies according to a barometric law. It has been found that the absorbing layers intersect at an angle of 17° and that the Sun is located near the axial plane of the absorbing layer of the Gould Belt and is probably several parsecs below the axial plane of the equatorial absorbing layer but above the Galactic plane. The model has been tested using the extinction of real stars from three catalogs.

*E-mail: georgegontcharov@yahoo.com

INTRODUCTION

There are regions with a comparatively high interstellar extinction far from the Galactic plane. For example, it can be seen on the $(J - K_s) - K_s$ diagrams for stars from the 2MASS catalog (Skrutskie et al. 2006) with accurate photometry in the J and K_s infrared bands presented in Fig. 1 that the reddening of stars in the regions at $l \approx 180^\circ$, $b \approx -15^\circ$ and $l \approx 0^\circ$, $b \approx +15^\circ$ is considerably higher than that in the symmetric regions at $l \approx 180^\circ$, $b \approx +15^\circ$ and $l \approx 0^\circ$, $b \approx -15^\circ$. Since the red dwarfs with $(J - K_s) \approx 0.9^m$, $K_s \approx 13^m$ and $M_{K_s} \approx 5$, thus located at distances up to 400 pc, reddened in these regions in the same way as distant stars, it should be recognized that the matter that caused this reddening is within 400 pc.

The model by Arenou et al. (1992), which approximates the mean extinction A_V for 199 regions of the sky by parabolas depending on the distance is still the best analytical 3D model of interstellar extinction within the nearest kiloparsec. This model reproduces adequately the observations within the nearest kiloparsec of the Sun. Its drawback is the absence of any physical explanation for the regularities in the observed extinction variations.

Figure 2a shows the dependence of extinction A_V on the Galactic longitude calculated using the model by Arenou et al. (1992) for a distance of 500 pc and Galactic latitudes $+15^\circ < b < +30^\circ$, $+5^\circ < b < +15^\circ$, $-5^\circ < b < +5^\circ$, $-15^\circ < b < -5^\circ$, $-30^\circ < b < -15^\circ$. The vertical bars indicate the accuracy of the model. The general, approximately sinusoidal longitude dependence of extinction near the Galactic equator is shown in Fig. 2b as $0.8 + 0.5 \sin(l + 20^\circ)$ (dashes). The Arenou model reflects but does not explain this dependence as well as the above-mentioned extinction features far from the Galactic plane: we see from Fig. 2a that the extinction is higher toward the Galactic center $+5^\circ < b < +30^\circ$ and toward the anticenter for $-30^\circ < b < -5^\circ$.

The accuracy of this model, i.e., the accuracy of predicting the extinction for a specific star, is, on average, from 20% to 50% at high Galactic latitudes and about 40% near the Galactic equator. This accuracy reflects the actual extinction variations from star to star in the same region of space: for example, for two neighboring stars 500 pc away; a scatter in extinction of $\pm 0.3^m$ at a typical extinction $A_V = 0.7^m$ is possible. Thus, modeling the extinction within the nearest kiloparsec, where each cloud, each Galactic structure, and even each star plays a role, is much more difficult than its modeling far from the Sun, where the high mean extinction smoothes out the role of individual

objects, and the extinction for a typical large region of space can be determined as, say, $5.0^m \pm 0.5^m$, i.e., with an accuracy of 10%. An *analytical* model of extinction within the nearest kiloparsec with a relative accuracy higher than that of the model by Arenou et al. (1992) is unlikely to be possible. To achieve a high accuracy of the extinction correction, it is more preferable to reveal specific absorbing clouds or to determine the individual extinction for each star from its highly accurate multiband photometry. However, a physically justified analytical model is important for analyzing large-scale structures within the nearest kiloparsec.

A Galactic structure, the Gould Belt, that lies outside the Galactic plane in the regions of the sky where an enhanced extinction is observed and that has a suitable size, several hundred parsecs, exists in the neighborhood of the Solar system. The Gould Belt and related Galactic structures, the Local Bubble and the Great Tunnel, were described by Gontcharov and Vityazev (2005 and references therein), Bobylev (2006 and references therein), and Perryman (2009, pp. 324-328 and references therein). The Gould Belt contains young stars and their associations. Stars are also formed here at present. The accompanying interstellar clouds can cause extinction. The extinction in the Gould Belt was first pointed out by Vergely et al. (1998).

In this paper, we tested the hypothesis that the interstellar extinction in the Gould Belt supplements the extinction along the Galactic plane and contributes significantly to the 3D pattern of extinction within the nearest kiloparsec.

THE MODEL

Figure 3 presents the relative positions of two layers of absorbing matter, the layer with halfthickness Z_A near the equatorial Galactic plane (below referred to as the equatorial layer) and the layer with half-thickness ζ_A in the Gould Belt. Denote the inclination of the Gould Belt to the Galactic plane by γ . The working coordinate system is defined by the observed coordinates of stars: the heliocentric distance r and the Galactic longitude l and latitude b . The Sun is at the origin of the working coordinate system and we do not consider its displacement relative to the Galactic plane, because it cannot be determined in the model under consideration. However, we consider the displacement of the axial plane of the equatorial layer relative to the Sun, Z_0 , and the analogous displacement for the absorbing layer of the Gould Belt, ζ_0 .

For clarity and comparison with the standard Galactic coordinate system, Fig. 3 shows the X' and Y' axes – the axes of a rectangular coordinate system in the axial plane of the equatorial layer. The X' axis is parallel to the direction toward the Galactic center and the Y' axis is parallel to the direction of Galactic rotation. We will designate the rotation of the highest point of the Gould Belt relative to the X' axis, i.e., the angle between the Y' axis and the line of intersection between the axial plane of the equatorial layer and the axial plane of the Gould Belt, as λ_0 .

The longitude λ and latitude β of a star relative to the axial plane of the Gould Belt can be calculated from its Galactic coordinates:

$$\sin(\beta) = \cos(\gamma) \sin(b) - \sin(\gamma) \cos(b) \cos(l) \quad (1)$$

$$\tan(\lambda - \lambda_0) = \cos(b) \sin(l) / (\sin(\gamma) \sin(b) + \cos(\gamma) \cos(b) \cos(l)). \quad (2)$$

The observed extinction A is approximated by the sum of two functions:

$$A = A(r, l, b) + A(r, \lambda, \beta), \quad (3)$$

each of them is represented by a barometric law (Parenago 1954, p. 265). The extinction in the equatorial layer is

$$A(r, l, b) = (A_0 + A_1 \sin(l + A_2)) Z_A (1 - e^{-r|\sin(b)|/Z_A}) / |\sin(b)|, \quad (4)$$

where A_0 , A_1 , and A_2 are the free extinction term, amplitude, and phase in the sinusoidal dependence on l , and the extinction in the Gould Belt is

$$A(r, \lambda, \beta) = (\Lambda_0 + \Lambda_1 \sin(2\lambda + \Lambda_2)) \zeta_A (1 - e^{-r|\sin(\beta)|/\zeta_A}) / |\sin(\beta)|, \quad (5)$$

where Λ_0 , Λ_1 , and Λ_2 are the free extinction term, amplitude, and phase in the sinusoidal dependence on 2λ . The assumption that the extinction in the Gould Belt has two maxima in the dependence on longitude λ was confirmed in our subsequent study. The extinction maxima in the Gould Belt are observed near the directions where the distance of the Belt from the Galactic plane is at a maximum, i.e., approximately in the directions of the Galactic center and anticenter.

Given the displacement of the Sun relative to the absorbing layers, Eqs. (4) and (5) transform to

$$A(r, l, Z) = (A_0 + A_1 \sin(l + A_2)) r (1 - e^{-|Z-Z_0|/Z_A}) Z_A / |Z - Z_0| \quad (6)$$

and

$$A(r, \lambda, \zeta) = (\Lambda_0 + \Lambda_1 \sin(2\lambda + \Lambda_2))r(1 - e^{-|\zeta - \zeta_0|/\zeta_A})\zeta_A/|\zeta - \zeta_0|. \quad (7)$$

The quantities $|Z - Z_0|/Z_A$ and $|\zeta - \zeta_0|/\zeta_A$ that are encountered in these formulas twice characterize the stellar position in the absorbing layers displaced relative to the Sun. We do not consider the displacement of the Sun relative to the center of the Gould Belt, because the accuracy of the data used is insufficient for this purpose.

As a result, we have the system of equations (3), one equation for each star. The observed extinction A is on the left-hand sides and the function of three observed quantities - r , l , and b - is on the right-hand sides. The solution gives 12 unknowns: γ , λ_0 , Z_A , ζ_A , Z_0 , ζ_0 , A_0 , A_1 , A_2 , Λ_0 , Λ_1 , Λ_2 . These are chosen so as to minimize the sum of the squares of the residuals of the left-hand and right-hand sides of Eqs. (3).

We can estimate some of the unknowns in advance. The inclination γ of the Gould Belt to the Galactic plane has been estimated by different researchers to be in the range 10° - 25° . Since the maximum height of the Gould Belt above the Galactic plane approximately coincides with the direction of the Galactic center, $\lambda_0 \approx 0^\circ$. The half-thickness of the absorbing layer Z_A is close to 100 pc (Parenago 1954). If the absorbing layer of the Gould Belt was produced by some “deformation” of the equatorial layer, then we can also assume the same halfthickness for it, i.e., $\zeta_A \approx 100$ pc. The displacements of the Sun relative to the absorbing layers Z_0 and ζ_0 are unlikely to exceed several parsecs; otherwise, this would be quite noticeable in the observational data. The combined mean extinction in the equatorial layer A_0 and the Gould Belt Λ_0 cannot differ too much from the universally accepted extinction in the near part of the Galaxy, 1.5^m kpc^{-1} .

COMPARISON OF THE MODELS

Given the large scatter of individual extinctions for stars within the nearest kiloparsec noted above, one might expect better agreement of the suggested analytical model and the model by Arenou et al. between themselves than with observations. Therefore, comparing the extinctions calculated using these models for the same stars is of great importance. In this case, the accuracy of the Galactic coordinates of stars is important. Consequently,

the best data are the coordinates of stars from the Hipparcos catalog (ESA 1997).

The model by Arenou et al. was used to calculate the extinctions for 89470 Hipparcos stars with parallaxes exceeding 0.0025 arcsec (i.e., located approximately in the Gould Belt). Based on these data, we obtained a solution to the system of equations (3) that is in best agreement with the model by Arenou et al. It is presented in the table as the HIP solution. Figure 4 shows how well the extinctions calculated from this solution agree with those inferred from the model by Arenou et al.: (a) for 89470 Hipparcos stars with parallaxes exceeding 0.0025 arcsec and (b) for 111444 stars with parallaxes exceeding 0.0005 arcsec.

The standard deviation of the differences between the extinctions calculated using the two models is designated in the table as $\sigma(A_G - A_{Arenou})$. It is 0.13^m . This confirms that the parabolas of the model by Arenou et al. can be replaced by the suggested analytical expression with two sine waves. In this case, the orientation of the Gould Belt, the thickness of the absorbing layers, the displacement of the Sun, and the total extinction correspond to the expected ones.

COMPARISON OF THE MODELS WITH OBSERVATIONS

Having ascertained that the two extinction models agree for a large number of Hipparcos stars, let us compare the models with the extinction data for real stars. Unfortunately, the extinction is low within 500 pc of the Sun, where the Gould Belt is located. Therefore, it is determined with a low relative accuracy, irrespective of the method of its determination. Consequently, there are few accurate extinction estimates for this region of space. In this paper, we consider three catalogs of stars with fairly accurate individual extinctions: for OB stars from the Hipparcos and Tycho-2 catalogs (Høg et al. 2000), the extinctions were determined from multiband photometry by Gontcharov (2008a; hereafter OB stars); for F and G dwarfs from the Geneva-Copenhagen survey of the solar neighborhood, the extinctions were estimated from Strömgren photometry (Nordström et al. 2004; hereafter GCS); and for various stars, the extinctions were derived from *UBV* photometry and spectral classification (Guarinos 1992; hereafter the V86 catalog, according

Table 1: Solutions of the system of equations (3)

	HIP	GCS	V86	OB_{hip}	OB_{rpm}	OB_{ph}
γ , deg	14 ± 2	17 ± 2	17 ± 2	17 ± 2	15 ± 2	19 ± 2
λ_0 , deg	-10 ± 2	-2 ± 7	-10 ± 3	-8 ± 3	-8 ± 3	-10 ± 3
Z_A , pc	70 ± 20	63 ± 14	100 ± 30	90 ± 20	60 ± 20	50 ± 20
ζ_A , pc	60 ± 20	26 ± 10	30 ± 30	50 ± 20	60 ± 20	45 ± 20
Z_0 , pc	15 ± 3	4 ± 11	-7 ± 10	16 ± 6	10 ± 6	0 ± 10
ζ_0 , pc	3 ± 3	0 ± 7	0 ± 10	6 ± 3	0 ± 3	0 ± 10
A_0 , mag pc $^{-1}$	1.2 ± 0.1	0.8 ± 0.1	2.0 ± 0.3	2.2 ± 0.1	1.9 ± 0.2	2.1 ± 0.2
A_1 , mag pc $^{-1}$	0.6 ± 0.1	0.3 ± 0.1	0.4 ± 0.3	0.6 ± 0.2	0.7 ± 0.1	0.9 ± 0.2
A_2 , deg	45 ± 5	39 ± 7	35 ± 10	37 ± 3	30 ± 4	32 ± 5
Λ_0 , mag pc $^{-1}$	1.0 ± 0.1	0.0 ± 0.1	0.2 ± 0.2	0.1 ± 0.1	0.5 ± 0.2	0.2 ± 0.2
Λ_1 , mag pc $^{-1}$	0.9 ± 0.1	0.4 ± 0.1	1.2 ± 0.4	1.0 ± 0.1	1.0 ± 0.1	0.8 ± 0.2
Λ_2 , deg	130 ± 5	129 ± 8	130 ± 10	131 ± 5	140 ± 5	133 ± 5
$\sigma(A_G - A_{Arenou})^m$	0.13					
$\sigma(A_{Obs} - A_{Arenou})^m$		0.11	0.27	0.26	0.37	0.35
$\sigma(A_{Obs} - A_G)^m$		0.06	0.28	0.22	0.38	0.35

to the Strasbourg database). We selected stars with Hipparcos parallaxes $\pi > 0.002$ arcsec from GCS and V86. For OB stars, we calculated the distances from their Hipparcos parallaxes as well as the photometric and photoastrometric distances (from reduced proper motions). Applying the extinction model to OB stars is also a check of how accurate the extinctions and distances calculated for them are.

Below, we will denote the observed extinction by A_{Obs} , the extinction from the model by Arenou et al. (1992) by A_{Arenou} , and the extinction from our analytical model by A_G .

GCS

The extinctions for GCS stars were determined from multiband Strömgen photometry. The solution of Eqs. (3) for 9996 of these stars with $\pi > 0.002$ arcsec from Hipparcos is presented in the table as the GCS solution. Here, the standard deviations of the $A_{Obs} - A_{Arenou}$ and $A_{Obs} - A_G$ differences are denoted by $\sigma(A_{Obs} - A_{Arenou})$ and $\sigma(A_{Obs} - A_G)$, respectively. We see that the suggested analytical model agrees better with the data than the model by Arenou et al. Unfortunately, the high accuracy of the extinctions determined from Strömgen photometry is compensated for by the closeness of the stars under consideration and, accordingly, by the low value of the extinction itself. In addition, the observed extinction is systematically lower than that calculated from both models: the mean observed extinction is $A_V = 0.04^m$, while the extinctions from the models by Arenou et al. and the suggested model are 0.12^m and 0.17^m , respectively. This may be the result of selection in favor of stars with lower extinctions in the GCS catalog.

V86

We determined the extinctions for V86 stars, which represent the entire variety of stellar types, from *UBV* photometry and spectral classification. The solution of Eqs. (3) for 9319 V86 stars with $\pi > 0.002$ arcsec from Hipparcos is presented in the table as the V86 solution. Contrary to popular belief, the present day spectral type-color index calibrations have an accuracy of no better than $\pm 0.3^m$ (or even $1^m \div 2^m$) due to the natural scatter of stellar characteristics (Perryman 2009, p. 215). The values of $\sigma(A_{Obs} - A_{Arenou})$ and $\sigma(A_{Obs} - A_G)$ given in the table confirm the crucial role of the natural scatter of stellar characteristics. The mean observed extinction is $A_V = 0.28^m$, the

extinction from the model by Arenou et al. is 0.25^m , and the extinction from the suggested model is 0.38^m .

OB stars

In this study, we are interested not in the spatial distribution of stars and other statistical characteristics of the sample of OB stars from Goncharov (2008a) but in the extinction, whose accuracy depends primarily on the accuracy of the multiband photometry used. Therefore, for this study, the stars with photometry less accurate than 0.05^m at least in one of the Tycho-2 and 2MASS bands under consideration were excluded from our sample: B_T , V_T , J , H , K_s . This should provide an accuracy of determining the reddening $E_{(B-V)}$ at a level of 0.1^m when four photometric quantities are used for this purpose. However, Gontcharov (2008a) calculated the extinction coefficient $R = A_V/E_{(B-V)}$ not for each star but for a region of space and, as Wegner (2003) showed, the standard deviation (natural scatter) of the coefficient R for OB stars in the same region of space is typically more than 0.3^m . Consequently, this is the expected accuracy of determining the extinctions for the OB stars considered here.

Instead of the relation $R = 2.8 + 0.18 \sin(l + 115^\circ)$ adopted by Gontcharov (2008a), here we use an apparently more plausible relation, $R = 2.65 + 0.2 \sin(l + 75^\circ)$. Like the previous one, it was derived by extrapolating the extinction law from the $(B_T - V_T) - (V_T - K_s)$ relation based on Tycho-2 and 2MASS photometry and is valid as an approximation at low Galactic latitudes. Obviously, a separate detailed study of the variations in R will be necessary.

To improve the accuracy, the stars with known spectral classification from the TST catalog (Wright et al. 2003) that did not belong to the O, B, and A0 types (the latter were retained, because they could actually belong to the B type due to the classification errors) were excluded from our sample. As a result of our analysis of the dependence of extinction on the effective wavelength, we adopted the following relation between the extinctions in the Johnson V band and the Tycho-2 V_T band in all our calculations: $A_V = 0.884A_{V_T}$. We rejected the stars with an observed extinction exceeding $1.1/(0.25 + |\sin(b)|)$; as a rule, these are peculiar late-type stars.

15670 stars remained in the final sample, instead of 37485 stars in the initial sample.

In Fig. 5, the observed extinction is plotted against the photometric

distance for Galactic latitudes $-5^\circ < b < +5^\circ$ in the first (a), fourth (b), and sixth (c) Galactic octants, which differ significantly by the pattern of extinction. We see a large natural scatter of individual extinctions in the first octant (more than 0.5^m), a much “quieter” picture in the fourth octant, and a low extinction and a standard deviation of less than 0.3^m in the sixth octant. The mean deviation of the individual stellar extinction from the analytical model also changes accordingly.

In Fig. 6, the extinction is plotted against the Galactic longitude. This dependence corresponds to the data of the model by Arenou et al. (1992) shown in Fig. 2a.

For 2472 Hipparcos OB stars with parallaxes exceeding 0.0025 arcsec, we obtained a solution presented in the table as the OB_{hip} solution.

Figure 7 shows the correspondence between the various extinctions for these 2472 OB stars: (a) A_{Obs} and A_{Arenou} ; (b) A_{Obs} and A_G calculated from the analytical model using photoastrometric distances; (c) A_{Arenou} and A_G calculated from the analytical model using Hipparcos parallaxes; and (d) A_{Obs} and A_G calculated from the analytical model using Hipparcos parallaxes. On the whole, we see good agreement.

The group of stars deviates from the bisector in Fig. 7c due to the asymmetry of the model by Arenou et al. (1992) in the Gould Belt, which is also seen in Fig. 2a: in the region with $l \approx 180^\circ$, $b \approx -15^\circ$, the extinction is $A_V \approx 2^m$, i.e., approximately twice that in the symmetric region with $l \approx 0^\circ$, $b \approx +15^\circ$, where $A_V \approx 1^m$. Our new analytical model gives approximately equal extinctions for these regions.

The group of stars deviating from the bisector in Fig. 7d consists mostly of supergiants and bright OB giants. The enhanced extinction in this case may be explained by the existence of an additional, noninterstellar extinction, say, in the envelopes of these stars.

For 7615 stars with photoastrometric distances less than 400 pc, we obtained a solution presented in the table as the OB_{rpm} solution. For 3054 stars with photometric distances less than 400 pc, we obtained a solution presented in the table as the OB_{ph} solution.

DISCUSSION

The following conclusions can be reached by comparing the solutions in the table.

(1) The differences in the solutions and the low accuracy of determining some of the unknowns confirm that the analytical models of extinction within the nearest kiloparsec are difficult to test, because there are no accurate extinction determinations for a large number of stars.

(2) The acceptable accuracy of the OB_{rpm} and OB_{ph} solutions as well as their agreement with the remaining solutions suggest that the photoastrometric and photometric distances can be used for an approximate calculation of the extinctions of stars based on the suggested analytical model if more accurate distances are unavailable.

(3) Comparison of $\sigma(A_{Obs} - A_{Arenou})$ and $\sigma(A_{Obs} - A_G)$ shows that the suggested model agrees with the observational data no more poorly than the model by Arenou et al. (1992).

(4) As expected, the two models under consideration are closer to each other than to the observational data due to the natural scatter of extinctions for individual stars.

(5) The values found for 10 unknowns (except A_0 and Λ_0) agree in all solutions.

(6) A_0 and Λ_0 vary from one solution to another, but their sum, along with the total calculated extinction, are approximately the same in all of the solutions except the GCS one. Only the total constant extinction rather than the constant extinction in each layer is reliably determined probably because of the low inclination of the Gould Belt to the Galactic plane and, accordingly, the narrow range of longitudes where the absorbing layers are separated. Since the extinction for GCS stars is low, we could not correctly estimate A_0 and Λ_0 . It is clear from physical considerations that A_0 and Λ_0 must be approximately equal. Therefore, we finally adopted $A_0 = 1.2^m$, $\Lambda_0 = 1.1^m$.

The final formulas to calculate the extinction from the suggested model with the best values of the unknowns found here are

$$(1.2 + 0.6 \sin(l + 35^\circ))r(1 - e^{-|Z-0.01|/0.07})0.07/|Z - 0.01|$$

and

$$(1.1 + 0.9 \sin(2\lambda + 135^\circ))r(1 - e^{-|\zeta|/0.05})0.05/|\zeta|,$$

where the longitudes l and λ are given in degrees; the distances r , Z , and ζ are given in kpc, and the resulting extinction is given in magnitudes. Figure 2b shows the dependence of extinction A_V on the Galactic longitude calculated from the suggested model for a distance of 500 pc and various Galactic

latitudes. The vertical bars indicate a relative accuracy of 40%. In Figs. 2a and 2b, we see good agreement between the models under consideration.

The extinction in the Gould Belt must hide the more distant stars. Indeed, analysis of the number of stars and the extinction for the OB stars under consideration with photometric distances from 400 to 800 pc shows that the number of stars is considerably larger in the southern (relative to the Sun and not relative to the Galactic equator!) hemisphere: 3841 versus 3415, while the extinction is higher in the northern hemisphere: 0.76^m versus 0.66^m . Figure 8 shows smoothed contour maps for the stars under consideration within 400–800 pc and $-36^\circ < b < +36^\circ$: (a) the extinction and (b) the number of stars. We see that the regions with a large number of stars have a comparatively low extinction and vice versa, i.e., the stars in the high-extinction regions are hidden. The high-extinction regions are located predominantly above the Galactic equator toward $l \approx 0^\circ$ and below it toward $l \approx 180^\circ$. This reflects the orientation of the Gould Belt. The stars remaining in the transparency windows do not show any distribution along the Gould Belt in Fig. 8b. As a result, contrary to the universally accepted approach, it is hard to judge the size and orientation of the Gould Belt from the apparent spatial distribution of its constituent stars. The Belt may have larger sizes than the commonly assumed ones.

The height of the Sun above the Galactic equator is usually estimated by counting the stars with positive and negative latitudes (Veltz et al. 2008). However, our study shows that the layer with the highest extinction may be several parsecs above the Sun, which, in turn, is approximately 13 pc above the Galactic plane (Gontcharov 2008b). At such a location, the northern stars, especially the distant ones, are hidden by extinction to a greater extent than the southern stars, and the star counts should give a height of the Sun above the Galactic plane larger than the true value, as, for example, 20 pc in Veltz et al. (2008). Obviously, when the height of the Sun above the Galactic plane is determined, the noncoincidence of this plane with the layer of the highest extinction should be taken into account.

CONCLUSIONS

This study has shown that there is absorbing matter both in the Galactic plane and in the plane of the Gould Belt. For this reason, the Gould Belt contributes significantly to the extinction for stars at moderate Galactic

latitudes, especially toward the Galactic center (at positive latitudes) and anticenter (at negative latitudes). The 3D model by Arenou et al. (1992) that represents the extinction as a parabola depending on the distance with various coefficients for 199 regions of the sky can be replaced by the sum of two sine waves that describe the extinction in the Galactic plane and in the plane of the Gould Belt. The absorbing layers were found to intersect at an angle of about 17° . This angle may be considered as the inclination of the Gould Belt to the Galactic equator. The angle between the line of intersection of the Gould Belt with the Galactic plane and the Y axis is about -10° . The Sun is probably several parsecs below the axial plane of the equatorial absorbing layer but above the Galactic plane.

The suggested analytical 3D extinction model agrees with the observed extinction for stars from the three catalogs considered and gives an extinction estimate for any star within 500 pc of the Sun (and possibly farther) based on its Galactic coordinates.

This paper opens a series of studies of the interstellar extinction in our Galaxy. In the future, we are going to construct an extinction model for much of the Galaxy using 2MASS photometry, which, as is shown Fig. 1, allows the reddening of stars in different directions and at different distances to be estimated.

ACKNOWLEDGMENTS

In this study, we used various results from the Hipparcos project and data from 2MASS (Two Micron All Sky Survey), a joint project of the Massachusetts University and the IR Data Reduction and Analysis Center of the California Institute of Technology financed by NASA and the National Science Foundation. We also used resources from the Strasbourg Data Center (France) (<http://cdsweb.u-strasbg.fr/>). This study was supported in part by the Russian Foundation for Basic Research (<http://www.rfbr.ru>) (project no. 08-02-00400) and in part by the “Origin and Evolution of Stars and Galaxies” Program of the Presidium of the Russian Academy of Sciences.

References

1. F. Arenou, M. Grenon, A. Gomez, *Astron. Astrophys.* **258**, 104 (1992).

2. V. V. Bobylev, *Pisma Astron. Zh.* **32**, 906 (2006) [*Astron. Lett.* **32**, 816 (2006)].
3. ESA, *Hipparcos and Tycho catalogues* (ESA, 1997).
4. G. A. Gontcharov, *Pisma Astron. Zh.* **34**, 10 (2008a) [*Astron. Lett.* **34**, 7 (2008a)].
5. G. A. Gontcharov, *Pisma Astron. Zh.* **34**, 868 (2008b) [*Astron. Lett.* **34**, 785 (2008b)].
6. G. A. Gontcharov and V. V. Vityazev, *Vestnik SPbGU*, Ser. 1, 3, 127 (2005).
7. J. Guarinos, in *Astronomy from Large Databases II, ESO Conference and Workshop Proc.*, No. 43, Ed. by A. Heck and F. Murtagh (1992), p. 301.
8. E. Høg, C. Fabricius, V.V. Makarov, et al., *Astron. Astrophys.* **355**, L27 (2000).
9. B. Nordström, M. Mayor, J. Andersen, et al., *Astron. Astrophys.* **418**, 989 (2004).
10. P. P. Parenago, *A Course on Stellar Astronomy* (GITTL, Moscow, 1954) [in Russian].
11. M. Perryman, *Astronomical application of astrometry* (Cambridge Univ., Cambridge, 2009).
12. M.F. Skrutskie, R.M. Cutri, R. Stiening, et al., *Astron. J.* **131**, 1163 (2006), <http://www.ipac.caltech.edu/2mass/releases/allsky/>.
13. L. Veltz, O. Bienayme, K.C. Freeman, et al., *Astron. Astrophys.* **480**, 753 (2008).
14. J.-L. Vergely, R. Freire Ferrero, D. Egret, et al., *Astron. Astrophys.* **340**, 543 (1998).
15. W. Wegner, *Astron. Nachr.* **324**, 219 (2003).
16. C.O. Wright, M.P. Egan, K.E. Kraemer, et al., *Astron. J.* **125**, 359 (2003).

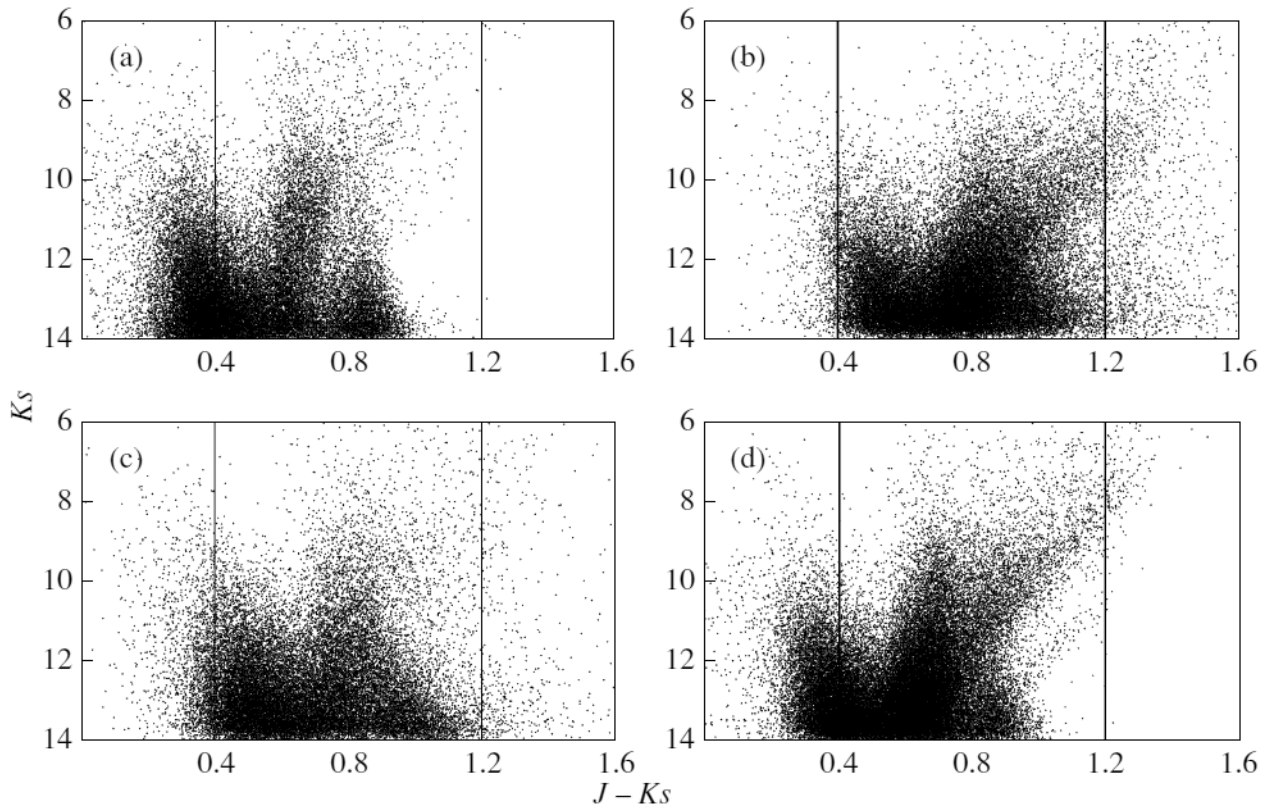


Figure 1: $(J - K_s) - K_s$ diagram for 2MASS stars with accurate photometry: (a) near $b = +15^\circ$, $l = 180^\circ$; (b) near $b = +15^\circ$, $l = 0^\circ$; (c) near $b = -15^\circ$, $l = 180^\circ$; (d) near $b = -15^\circ$, $l = 0^\circ$.

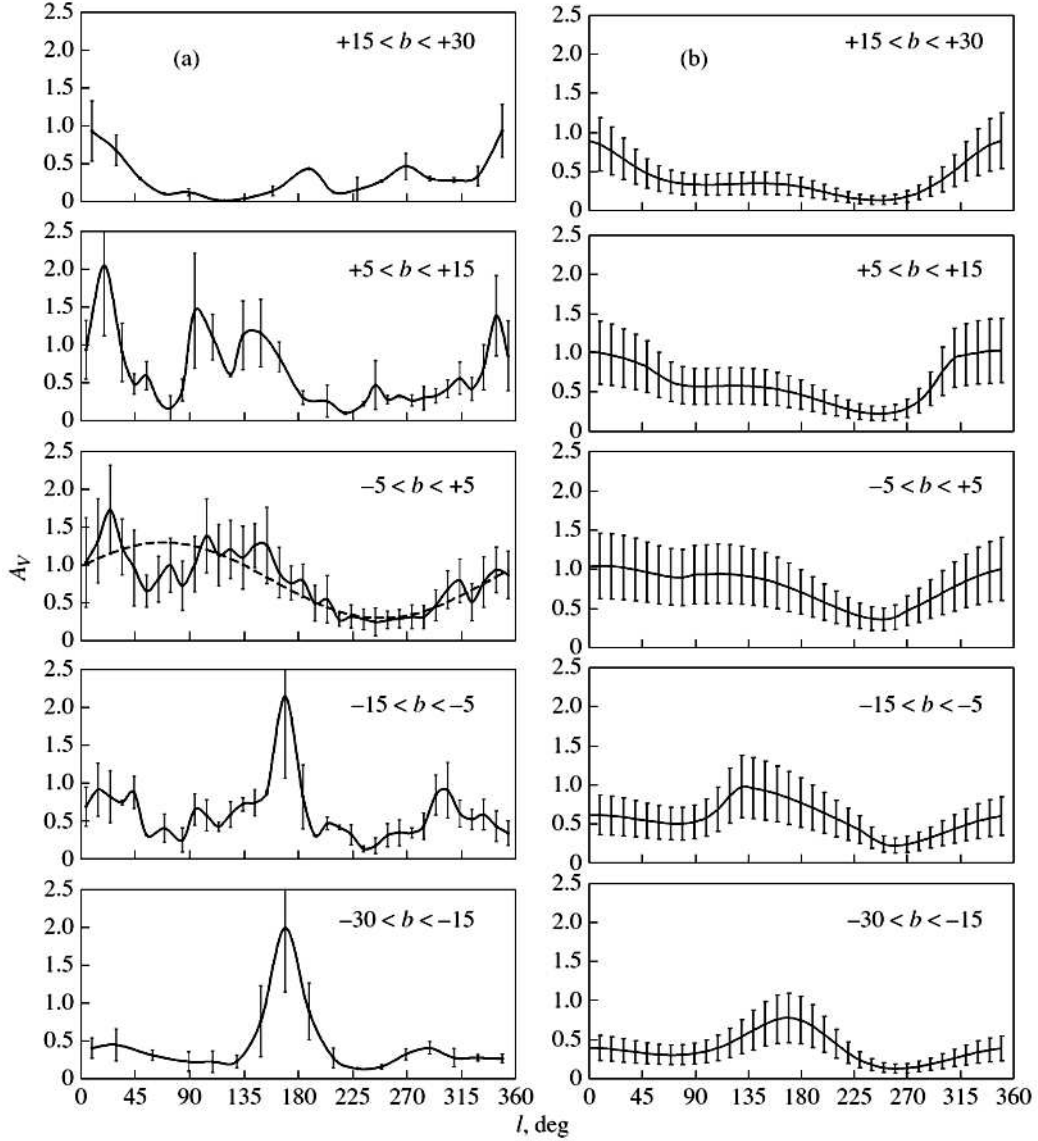


Figure 2: Extinction A_V versus Galactic longitude at a distance of 500 pc from the Sun for various Galactic latitudes: (a) according to the model by Arenou et al. (1992); (b) according to the model suggested here. The dashes indicate the dependence $0.8 + 0.5 \sin(l + 20^\circ)$. The vertical bars indicate the accuracy of the model by Arenou et al. (1992) and a relative accuracy of 40% for the suggested model.

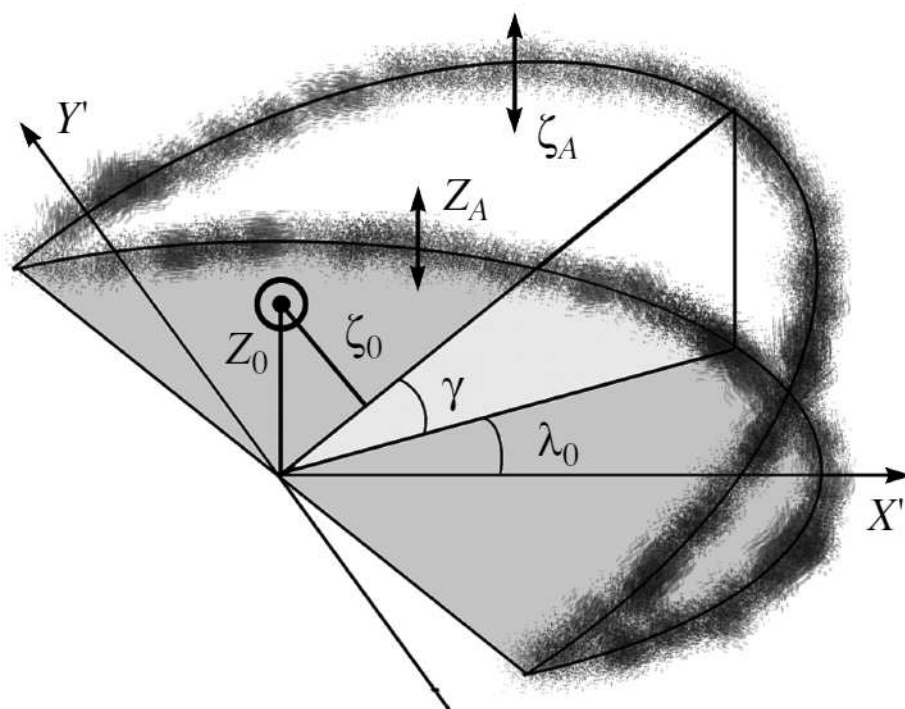


Figure 3: Relative positions of two absorbing layers.

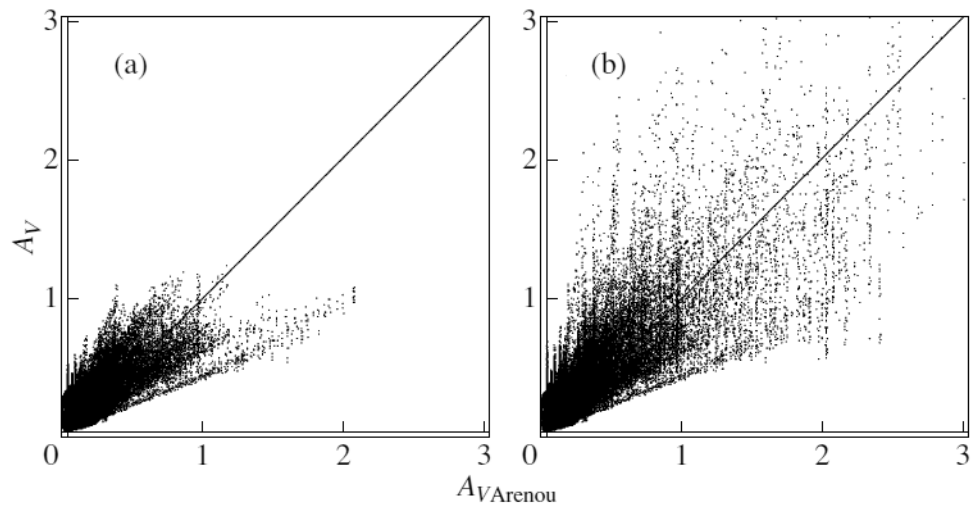


Figure 4: Correspondence between the extinctions calculated here and those inferred from the model by Arenou et al. (1992) for 89470 Hipparcos stars with parallaxes exceeding 0.0025 arcsec (a) and for 111444 stars with parallaxes exceeding 0.0005 arcsec (b).

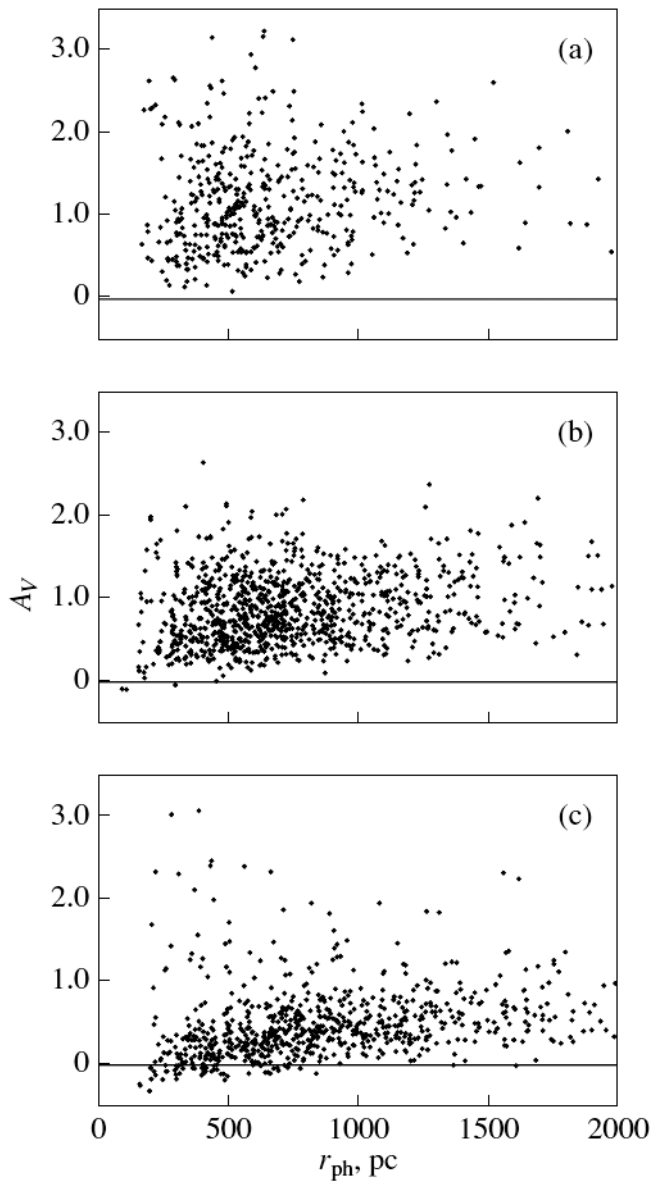


Figure 5: Extinction versus photometric distance for the OB stars under consideration in the region $-5^\circ < b < +5^\circ$ for (a) $0^\circ < l < 45^\circ$, (b) $135^\circ < l < 180^\circ$, and (c) $225^\circ < l < 270^\circ$.

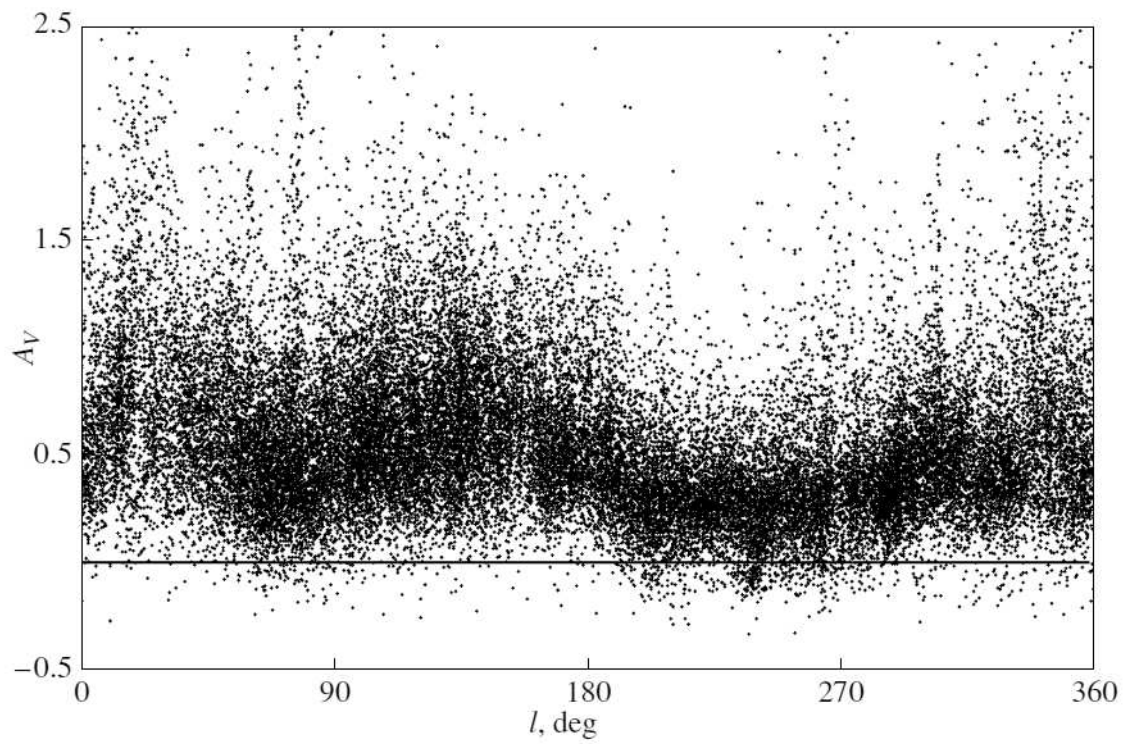


Figure 6: Extinction versus Galactic longitude for the OB stars under consideration.

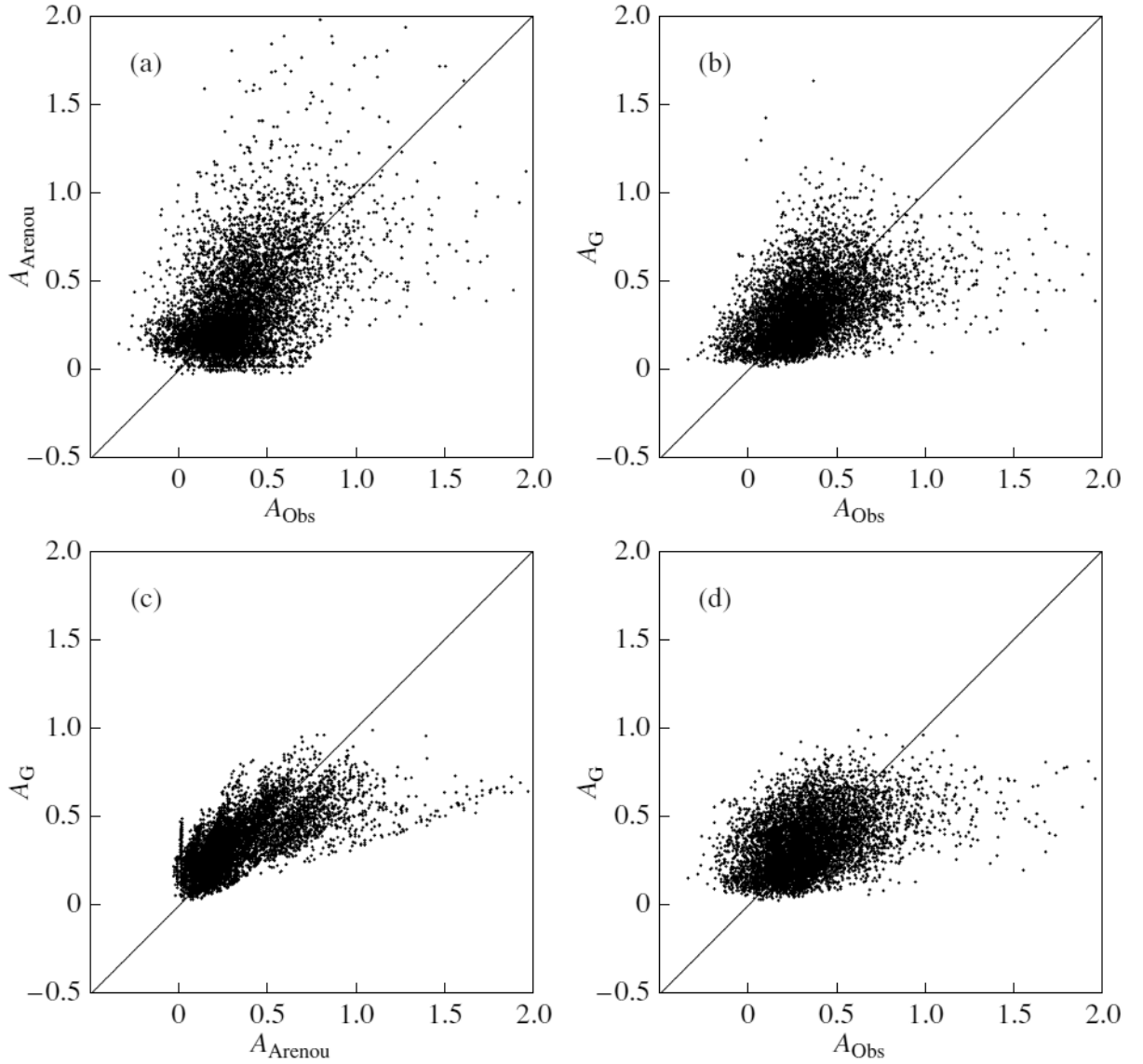


Figure 7: Correspondence between the various extinctions for 2472 Hipparcos stars: (a) the observed extinctions and those from Arenou et al. (1992); (b) the observed extinctions and those calculated using photoastrometric distances; (c) the extinctions from Arenou et al. (1992) and those calculated using astrometric distances; (d) the observed extinctions and those calculated using astrometric distances.

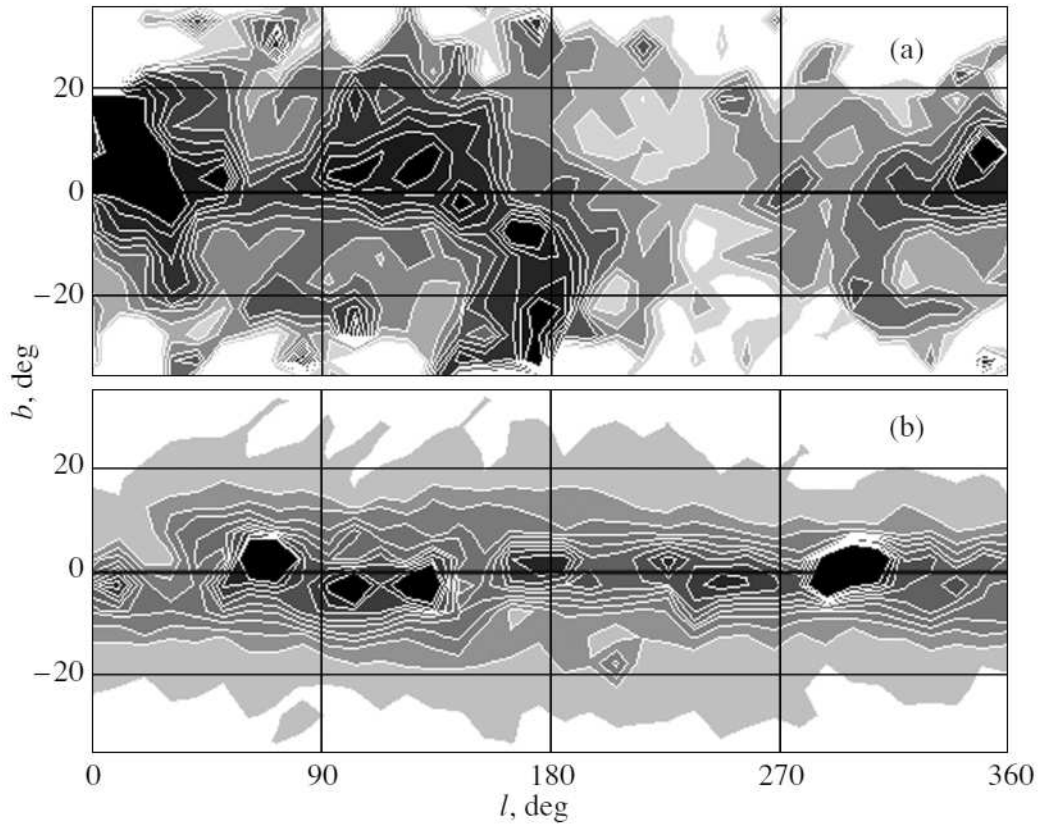


Figure 8: Smoothed contour maps for the OB stars under consideration within 400–800 pc and $-36^\circ < b < +36^\circ$: (a) the extinction and (b) the number of stars.